

Modeling of Damage Behavior of Cast Aluminum Components Taking into Account Porosity Effects

Dong-Zhi Sun¹, Andrea Ockewitz¹, Florence Andrieux¹, Herbert Klamser²

¹Fraunhofer Institute for Mechanics of Materials, Woehlerstrasse 11, Freiburg, Germany

²Porsche AG, Porschestrasse, Weissach, Germany

The analysis of the damage behavior of cast components is very complex, since local mechanical properties in the components are inhomogeneous as a consequence of spatial distribution of microstructure e.g. pore and grain sizes, arm spacing of secondary dendrites. In this work the flow stress and fracture strain were determined for different positions in a die cast component. Tension, shear and compression tests on different specimens cut from the component were performed to determine the dependence of the fracture strain on stress triaxiality. A damage model was developed to take into account the influence of triaxiality and initial porosity on damage. Component tests and simulations were conducted to validate the numerical method. The distribution of porosity in the component calculated by casting simulation was transferred to the component simulation. It was found that material characterization under different loading types and damage modeling with consideration of the influence of triaxiality and porosity are necessary for a reliable component simulation.

Keywords: *Characterization, damage model, porosity, simulation, component tests.*

1. Introduction

Aluminum pressure die cast components are widely used in vehicle constructions due to light weight requirements and economical benefits e.g. reduction of production steps for complex components in one process. However, the complex geometries of die cast components with inhomogeneous microstructure and porosity result in a higher risk of fracture, as there are high stress and strain concentrations at notch root and the positions with higher porosity show a much lower fracture strain [1]. The inhomogeneity of mechanical properties makes an analysis of the damage behavior of die cast components more complex. Both the influence of stress state on damage development and the large scatter of local material properties have to be considered in the component simulation.

A meaningful way for the consideration of the influence of die cast processes on local properties in a crash analysis is a coupling between casting simulation and crash simulation. In the work [1] the distribution of shrinkage porosity in an aluminum die cast component was calculated by casting simulation and verified by CT scans. It was found that the fracture strain in the region of tension is significantly reduced by increasing porosity whereas it is independent of the porosity level in the region of shear. The numerical investigation [2] shows that not only the spatial distribution of porosity but also microstructure e.g. grain sizes and arm spacing of secondary dendrites and residual stresses in an aluminum die cast component can be calculated by casting simulation. Until now there are only a few investigations about characterization and modeling of the influences of porosity and loading type (triaxiality) on the fracture behavior of aluminum die cast components. In the work [3] an interesting model was suggested to describe the influence of porosity and triaxiality by extending the Gurson-Model [6] for shear region. Another approach [4] was suggested by using the Gologanu model [7] and two fracture criteria.

In this work the effects of triaxiality and porosity on the fracture behavior of an aluminum die cast component were characterized under different load types and modeled with mapping of the

results of casting simulation onto the component model. Component tests were performed and numerical predictions based on different damage models were compared.

2. Material characterization and damage modeling

2.1 Characterization under tension, compression and shear

An aluminum die cast component was experimentally characterized with small specimens cut from different positions (Fig. 1) under tension, compression and shear. The fracture modes of the different specimens are shown in Fig. 2. This aluminum die cast alloy fails not only under tension but also under compression. However, the fracture strains under tension are much smaller than under compression (Fig. 3). As expected from a cast alloy the scatters of strength and fracture strain are large. Both the modified Iosipescu specimen (d in Fig. 2) and double-notched shear specimen (e in Fig. 2) were used to characterize shear fracture. It can be recognized from Fig. 2 that both tension fracture and shear fracture are possible in the double-notched shear specimen.

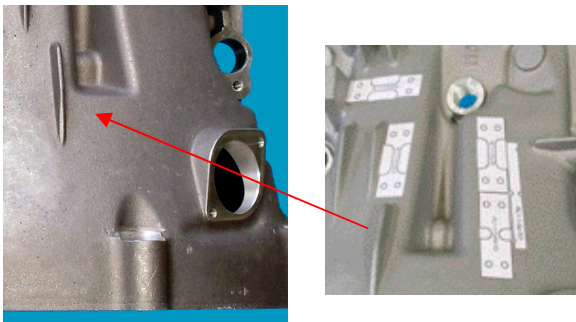


Fig. 1: Aluminum die cast component and example for specimen extraction

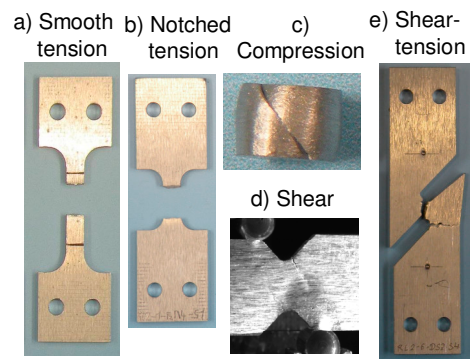


Fig. 2: Different specimens after tests

The fracture strains and the corresponding triaxialities were determined by modelling the specimen tests. The triaxiality is defined as the ratio of the mean stress σ_m to the von Mises effective stress σ_e . The values of triaxiality for shear, uniaxial tension and biaxial tension are zero, one third and two thirds, respectively. Since local strains and triaxiality are not homogeneous in the specimens due to stress gradients or localization of deformation, the critical values were taken from the first damaged elements at the measured fracture displacement. The values presented by symbols in Fig. 4 were determined in this way. The arrow on the triangle symbol near triaxiality of zero indicates that the fracture strain for this triaxiality must be higher since damage in the shear specimen does not initiate at this position.

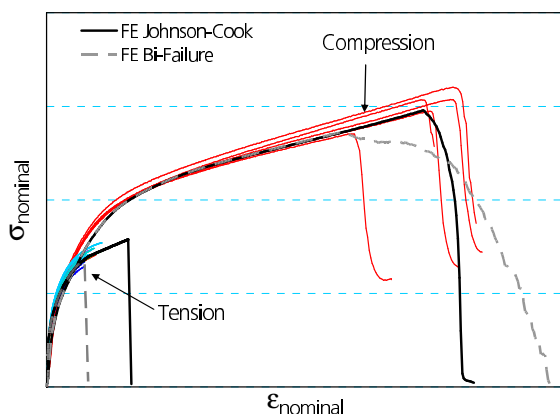


Fig. 3: True stress vs. true strain curves of tension and compression specimens

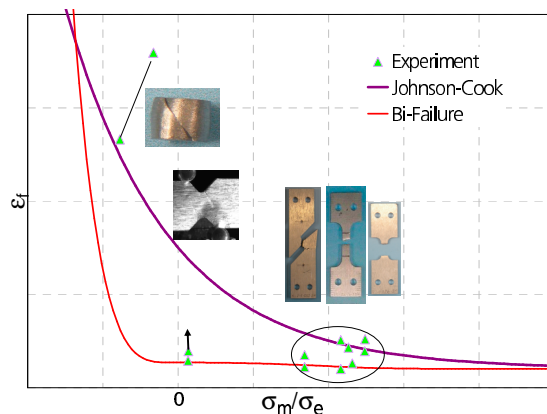


Fig. 4: Fracture strain vs. triaxiality from experiments and two damage models

2.2 Damage model (Bi-Failure)

The damage model (Bi-Failure) proposed in this work is based on a fracture strain criterion. The fracture strain ε_f is defined as a function of the stress triaxiality $T = \sigma_m / \sigma_e$. The difference to the Johnson-Cook type fracture criterion [5] is that the fracture strain does not decrease monotonically with increasing triaxiality. The domain of triaxiality is divided into two regions for dimple rupture at high triaxialities and shear failure at low triaxialities. Above a triaxiality T_{trans} (which is a material parameter and is expected to be about 0.3) the failure curve proposed by Johnson-Cook Eq. (1) is used which involves three material parameters d_1 , d_2 and d_3 . Below T_{trans} an empirical polynomial curve Eq. (2) is proposed with a minimum at $T=0$.

$$T > T_{trans} \quad \varepsilon_f = (d_1 + d_2 \exp(-d_3 T)) \quad (1)$$

$$T < T_{trans} \quad \varepsilon_f = d_{shear1} + d_{shear2} |T|^{m_2} + d_{shear3} \langle -T \rangle^{m_3} \quad (2)$$

The third term in Eq. (2) is introduced to define an asymmetry in the failure strain with respect to the triaxiality, especially to account for different failure strains in tension and in compression, eventually no failure in compression at all. In Eq. (2) $\langle \cdot \rangle$ denotes the Macauley bracket which returns the argument when positive and zero otherwise. In Eq. (2) d_{shear1} , d_{shear3} , m_2 and m_3 are material parameters for the shear region ($T < T_{trans}$). The value d_{shear2} is no free parameter and should be calculated to ensure the continuity of the failure strain function at T_{trans} . The parameter d_{shear3} is calculated in the model by using the fracture strain under uniaxial compression ($T = -1/3$). Fracture occurs when the cumulative damage parameter D defined by Eq. (3) reaches the critical value of 1. Johnson-Cook [5] proposed a linear damage accumulation. A more general non-linear damage accumulation is used here:

$$\dot{D} = \frac{n}{\varepsilon_f^n} \varepsilon_p^{n-1} \dot{\varepsilon}_p \quad (3)$$

In Eq. (3) ε_p denotes the equivalent plastic strain and the exponent n is a parameter controlling the damage evolution. For proportional loading the integration of Eq. (3) leads to $D = (\varepsilon_p / \varepsilon_f)^n$. The damage curves determined for the aluminum die cast alloy according to the Johnson-Cook model and the Bi-Failure model are compared in Fig. 4.

A Gurson-type relation is used to describe the effect of porosity on the yield stress σ_y :

$$\sigma_y = \sqrt{1 - q_1 f_0} \sigma_y^0 \quad (4)$$

In Eq. (4) f_0 denotes porosity, σ_y the yield stress for the porosity f_0 , σ_y^0 the yield stress of the full material and q_1 is a material parameter. To describe the effect of the porosity on the failure strain in a uniaxial tensile test the relation Eq. (5) is used:

$$\varepsilon_f = \varepsilon_f^0 (1 - q f_0)^n \quad (5)$$

In Eq. (5) ε_f denotes fracture strain for the porosity f_0 , ε_f^0 the failure strain of the full material and q and n are two material parameters. Due to lack of experimental data the relation Eq. (5) was used to scale the fracture strain for positive triaxialities. The porosity influence in the region of negative triaxialities was scaled differently so that the porosity has no effect under uniaxial compression.

The parameters in Eq. (4) and (5) were determined by evaluating the flow stresses and fracture strains of tensile specimens taken from different positions in the component and the corresponding values of porosity calculated by casting simulation. Fig. 5 shows the true stress vs. true strain curves for different porosities. The color lines are from experiments and the grey lines are calculated from Eq. (4) and (5). With increasing porosity the flow stress and especially the fracture strain decrease significantly. Metallographic examination of fracture surfaces of the specimens gives evidence that more pores and shrinkage cavities were observed in the specimens which show a lower fracture strain. As an example Fig. 6 shows the fracture surface of a smooth flat specimen with different sizes of pores. Since the fracture of the specimens was triggered by large pores which are

statistically distributed, there is a large scatter of the strength and the fracture strain.

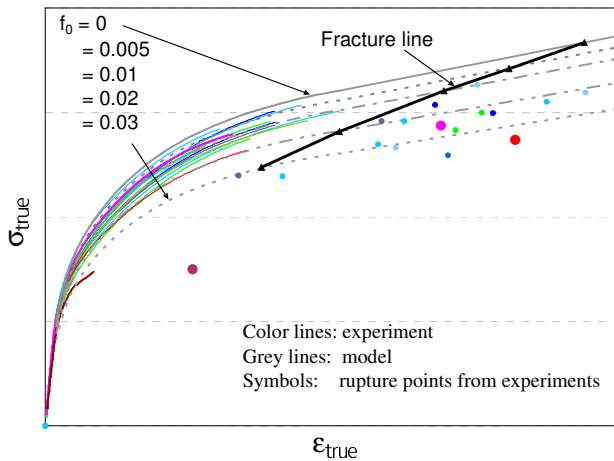


Fig. 5: Influence of porosity on flow stress and fracture strain

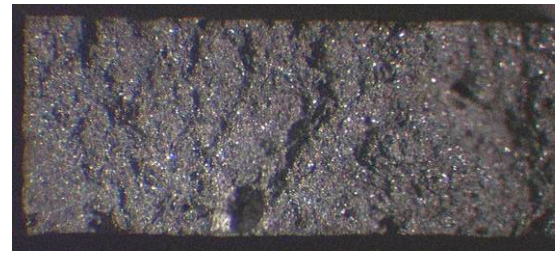


Fig. 6: Fracture surface of a smooth flat specimen with different sizes of pores

2.3 Simulation of different specimen tests

Both the damage model described above and the Johnson-Cook model were used to simulate all specimen tests performed in this work. In the simulation of specimen tests the influence of porosity on fracture strain and flow stress (Eq. (4) and (5)) were not taken into account. The damage parameters of the Bi-Failure model d_1 , d_2 and d_3 for the region $T > 1/3$ were determined by fitting the fracture strains of smooth and notched tension specimens. The damage parameters for the range $T < 1/3$ were obtained by fitting the fracture strains of shear-tension and compression specimens. The damage curves determined for the Johnson-Cook model and the Bi-Failure model are given in Fig. 4. The main difference between both damage curves lies in the region of triaxialities from $-1/3$ to $1/3$. Since no experimental data for fracture strain under pure shear ($T=0$) are available, the consequence of the difference can only be checked in component simulations. Fig. 7 compares the measured and calculated nominal stress vs. nominal strain curves of tension and compression tests. In both load cases the calculated fracture initiation results in a significant drop of load. The fracture initiations according to the Johnson-Cook model are slightly later than those from the Bi-Failure model. Fig. 8 shows the deformation and damage patterns of the tension and compression specimens calculated with the Johnson-Cook damage model.

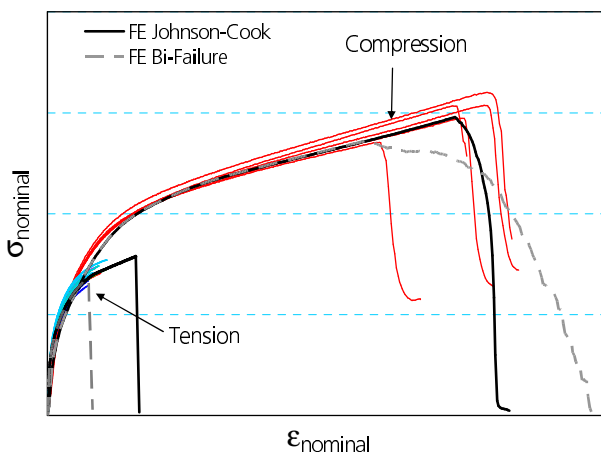


Fig. 7: Measured and calculated nominal stress vs. nominal strain curves under tension and compression

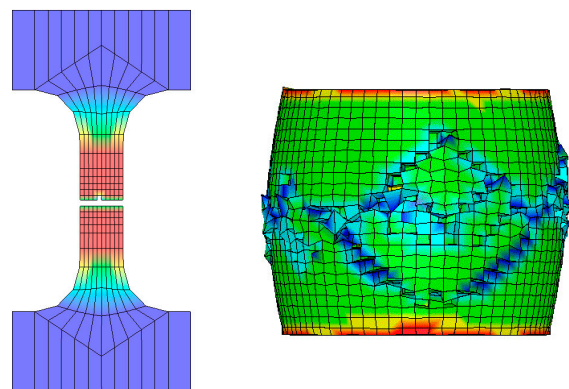


Fig. 8: Calculated damage pattern of tension and compression specimens

3. Component tests and simulation

For a validation of the damage models component tests on the aluminum component were performed under static compression. Damage initiation occurs in the basement region (Fig. 9a) at a stamp displacement of 4 mm. The measured load vs. displacement curves (green) are given in Fig. 10. The scatter in the global responses and local damage behavior is relatively small.

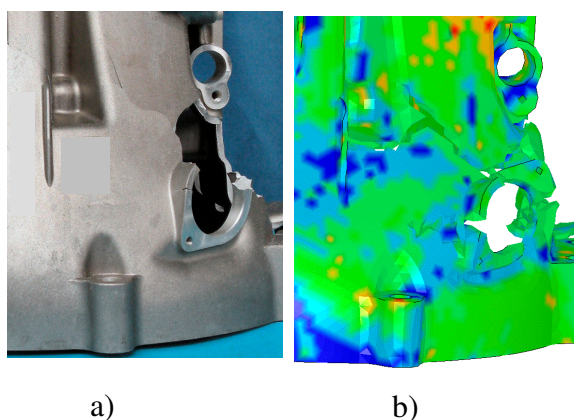


Fig. 9: Damage pattern in experiment a) and in simulation with Bi-Failure model b)

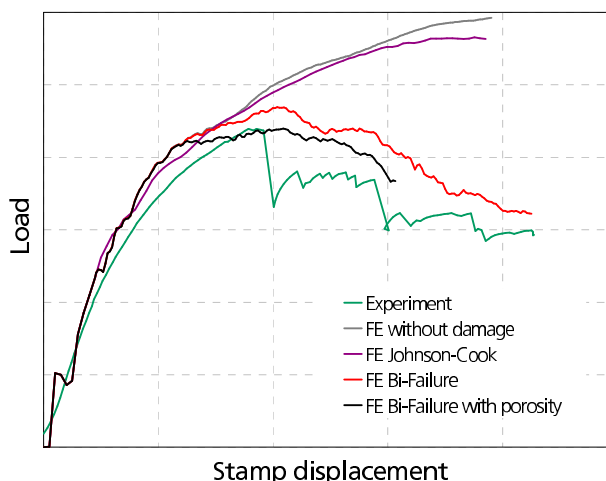


Fig. 10: Measured and calculated load vs. stamp displacement curves of component tests

The component model was generated with tetrahedral elements. The contact surfaces between the stamp, the component and the bottom were modeled with contact elements. Both damage curves shown in Fig. 4 were used for component simulations. Additionally, a simulation with consideration of the influence of porosity on the flow stress and fracture strain was conducted. The distribution of shrinkage pores in the component was determined by casting simulations which were performed at Fraunhofer IFAM. Samples cut from several positions in the component were investigated with CT scans at Fraunhofer IFAM. The numerical predictions of porosity were confirmed by the CT scans. Since the FE models for casting simulation and component simulation are different in element sizes and geometry due to modeling of the gating system in the casting model, the distribution of porosity calculated from the casting simulation was mapped onto the component model. The values of porosity were used in the component model for the Bi-Failure model to calculate the corresponding flow stress and fracture strain according to Eq. (4) and Eq. (5).

The load vs. stamp displacement curves from experiments and simulations with different damage models are compared in Fig. 10. The Johnson-Cook model with the associated damage curve shown in Fig. 4 underestimates remarkably damage development and cannot predict the load drop caused by damage. The results from the Johnson-Cook model are similar to those obtained by simulation without damage modeling. The simulation with Bi-Failure model can predict the course of the load vs. displacement curves in a satisfactory way. The simulation taking into account porosity effects delivers the best agreement with the experimental results.

4. Conclusion

The deformation and damage behavior of an aluminum die cast component was characterized under tension, shear and compression. A damage model was developed to model the influence of triaxiality and porosity on fracture strain. Component tests were performed to validate the applied damage models with the associated damage curves. The distribution of porosity calculated by casting simulation was mapped to the component model to take into account the effect of porosity on damage behavior of the component. It was found that the scatters of the flow stress and fracture

strain are very large and the fracture strain depends strongly on triaxiality. The component simulations with different damage models show that the application of a suitable damage model and the determination of the corresponding damage curve are essential steps for a reliable prediction of damage behavior of aluminum die cast components.

The influences of porosity and triaxiality on fracture strain are overlaid and it complicates the validation of the damage models describing both effects. Further investigations are necessary for improvement of the applied damage model concerning porosity influence on damage development under different load conditions especially under shear. The casting simulation can also be improved concerning prediction of porosity. Not only shrinkage pores but also gas pores should be treated in casting simulations.

Acknowledgement

We are grateful to Fraunhofer IFAM and Georg Fischer AG for the casting simulations and useful discussions.

References

- [1] C. Leppin, H. Hooputra, H. Werner, S. Weyer, R.V. Büchi, VIII International Conference on Computational Plasticity, COMPLAS VIII, E. Oñate and D. R. J. Owen (Eds), Ó CIMNE, Barcelona, 2005.
- [2] E. Flender, G. Hartmann, GIESSEREI 92 03/2005, 38-49.
- [3] K. Nahshon, J.W. Hutchinson, Euro. J. Mech. A/Solids, 2008, 27, 1-17.
- [4] F. Andrieux, D.-Z. Sun, to be published in International Journal of Materials Research.
- [5] G.R. Johnson, W.H. Cook, Engineering Fracture Mechanics, vol.21, No.1, 1985, pp.31-48.
- [6] A. Needleman, V. Tvergaard, J. Mech. Phys. Solids 35, 1987, S. 151-183.
- [7] M. Gologanu, J.B. Leblond, J. Devaux, J. Mech. Phys. Solids 41, 1993, S. 1723-1754.